

The dynamics of NO radical formation in the UV 266 nm photodissociation of nitroethane

Yamin Li ^{a,c}, Julong Sun ^a, Keli Han ^{a,*}, Guozhong He ^a, Zhuangjie Li ^b

^a State Key Laboratory of Molecular Reaction Dynamics, Dalian Institute of Chemical Physics, Chinese Academy of Science, Dalian 116023, China

^b Department of Chemistry and Biochemistry, California State University Fullerton, Fullerton, CA 92834–6808, United States

^c College of Environmental Science and Engineering, Department of Applied Chemistry, Dalian Jiaotong University, Dalian, Liaoning 116028, China

Received 5 November 2005; in final form 12 January 2006

Available online 17 February 2006

Abstract

Photodissociation of gaseous nitroethane at 266 nm has been studied by monitoring the NO($X^2\Pi$) product using laser-induced fluorescence technique. Rotational state distributions of the NO($X^2\Pi_{1/2}$ and $X^2\Pi_{3/2}$, $v'' = 0$) photofragment have been measured and characterized by Boltzmann temperature of 810 ± 100 K. Only the NO photoproduct in $v'' = 0$ state can be observed in the present work. The geometries of the nitroethane, the ethyl nitrite and the transition state connecting the two isomeric structures have been investigated using ab initio method. The photodissociation dynamics of nitroethane is discussed on the basis of experimental observation and calculation results.

© 2006 Elsevier B.V. All rights reserved.

1. Introduction

Studies of photodissociation dynamics of nitro compounds [1–29] are of much interest because these molecules, upon UV irradiation, can dissociate through different pathways including simple bond cleavage, concerted molecular dissociation, and rearrangement or elimination through cyclic transition states, which may compete with each other [1]. There has been an extensive review on the chemistry of nitrocompounds [16], and previous understanding of the various primary and secondary reactions of nitroalkanes has focused on acquiring knowledge of thermochemistry and thermal decomposition of these compounds. The main experimental efforts on photodissociation of these molecules have concentrated on the determination of distributions of internal-state distribution and the translational-energy distributions of the fragments [7,8]. Direct detection of the primary photodissociation fragments following excitation of

nitromethane has been accomplished by several groups [2,3,6,14]. Excitation of nitromethane at 280 nm leads to three dissociation channels: (1) the production of NO₂ and methyl radical, (2) the formation of oxygen atoms in conjunction with nitrosomethane, CH₃NO, and (3) the production of NO and methoxy radicals.



The dominant channel of nitromethane photolysis at 200 nm is the production of electronically excited NO₂ and methyl radicals. For larger nitroalkanes, C_nH_{2n+1}NO₂ with $n > 1$, the most interesting feature of their chemistry is the number of energetically possible dissociation pathways. It is known that their lowest energy pathway is HONO elimination to produce stable alkene [12]. Other possible channels for nitroalkane photodissociation include NO₂ and alkyl radical formation, as well as NO and alkoxy radical production.

Very limited information is available in literature regarding the photodissociation of nitroalkanes with two

* Corresponding author.

E-mail addresses: ymli@dicp.ac.cn (Y. Li), klhan@dicp.ac.cn (K. Han).

or more carbon atoms. For nitroethane, $C_2H_5NO_2$, the infrared multiple photon dissociation (IRMPD) of nitroethane at 9.6 μm had been researched by Wodtke et al. [3]. However, the UV photodecomposition of nitroethane is less studied. This may be due to the fact that the UV photoexcitation dynamics of nitroethane is very complicated. On the other hand, the competition among various energetically allowed channels makes it an interesting system for experimental and theoretical studies. The UV absorption spectrum of nitroethane consists of two smooth, broad bands centered roughly at 280 and 200 nm [12]. The band at longer wavelength has been assigned to a $\pi^* \leftarrow n$ transition that is located on the NO_2 functional group, while the feature at 200 nm is assigned to a $\pi^* \leftarrow \pi$ transition also located on the NO_2 chromophore [12]. In this Letter, we report our investigation of photolysis of $CH_3CH_2NO_2$ at 266 nm



with focus on the detection of NO from the photolysis. We also performed the ab initio study on the reaction dynamics for reaction (6). We will discuss the photodissociation dynamics of nitroethane leading to NO observation based on our ab initio computational results.

2. Experimental and theoretical approaches

The dissociation pulsed Nd: YAG laser (Quanta-Ray DCR-3G) beam and the probe laser beam were propagated collinearly and were focused on the center of a fluorescence cell, and the probe pulse was delayed by ca. 20 ns optically with respect to the dissociation pulse. The light from the fourth harmonic of a Nd: YAG laser (Quanta-Ray DCR-3G) at 266 nm provided the photolysis pulses at a repetition rate of 10 Hz. The probe beam was generated by frequency doubling a YAG (Quanta-Ray GCR-3G) laser pumped dye laser (Lumonics HD-500). The photolyzing beam and probe beam, which were slightly focused by a lens of $f = 0.75$ m, had a diameter of ~ 3 and ~ 1 mm at the observation point, respectively. Saturation effect was avoided by keeping low laser pulse energies of 1.4 mJ for the photolyzing beam and < 0.1 mJ for the probe beam. The NO LIF signal was found to be linearly proportional to the laser power, and did not exhibit a leveling off at high laser powers. The fluorescence resulted from NO at the $A^2\Sigma^+(v' = 0) \leftarrow X^2\Pi(v'' = 0)$ transition was detected by a photomultiplier tube (PMT, Hammamatsu R 1460) at a right angle to both the gas beam and the two counter propagating laser beams. The PMT signal was passed through a band-pass filter (centered at $\lambda = 236.5$ nm, bandwidth ≈ 10 nm), and then averaged with a boxcar integrator (Stanford SR250). About 100 mtorr of gaseous nitroethane was flowed through a reaction cell, which was constantly monitored

by a pressure gauge. Only the NO photoproduct in $v'' = 0$ state can be observed in this work. Experiments were carried out at 298 ± 3 K. The polarization effects were not taken into consideration.

In an effort to unravel the possible photodissociation mechanism of nitroethane, we also employed ab initio molecular orbital theory to investigate the isomerization process of nitroethane. All calculations were carried out using the GAUSSIAN98 program package [30]. The geometries of the nitroethane, the ethyl nitrite and the transition state between the two isomeric structures were fully optimized using Møller–Plesset correlation energy correction truncated at second-order (MP2) theory in conjunction with 6-31G** basis set (MP2/6-31G**). Vibrational frequencies were calculated at the same level of theory for verification of structural optimization and for computation of zero point energy. Single point energies of nitroethane the ethyl nitrite and the transition state were calculated at MP4/6-311G** level, and the best estimate of energetics was made by adding zero point energy correction to the MP4/6-311G** single point result (MP4/6-311G**//MP2/6-31G** + ΔZPE).

3. Results and analysis

Investigation of the internal-state distribution of the NO $X^2\Pi$ fragment was carried out via one-photon laser-induced fluorescence (LIF) technique monitoring the NO $A^2\Sigma^+(v' = 0) \leftarrow X^2\Pi(v'' = 0)$ transition. Fig. 1 shows the region of the NO $A^2\Sigma^+(v' = 0) \leftarrow X^2\Pi(v'' = 0)$ excitation spectrum at 223.75–227.15 nm. In order to assign the J'' values of NO ($X^2\Pi$) populated in the dissociation process precisely the experimental spectra were compared with the simulated NO excitation spectra calculated from the known spectroscopic constants and Hönl–London factors [31]. Since the selection rules for one-photon absorption allow transitions with $\Delta J = 0, \pm 1$, only P , Q , and R branches are observed. Furthermore, the 2I and $^2\Sigma^+$ states are split by spin–orbit and spin–rotation interactions causing each band to consist of 12 rotational sub-branches [31].

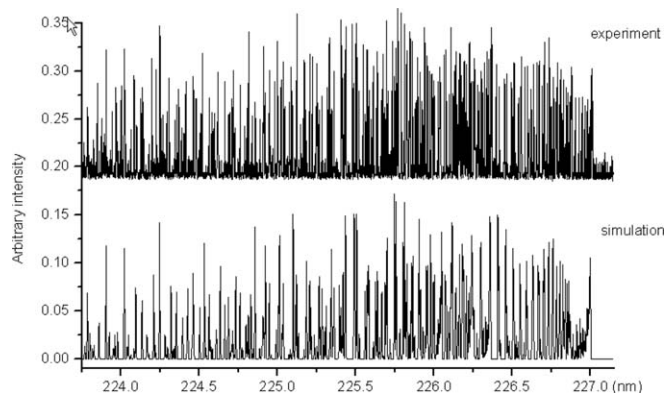


Fig. 1. Portion of the $^2\Sigma^+(v' = 0) \leftarrow ^2\Pi(v'' = 0)$ band of the one-photon LIF spectrum of the NO fragment from $C_2H_5NO_2$ photodissociation at 266 nm. Upper spectrum, experiment; lower spectrum, simulation.

The intensity of the spectra can be described by the equation as follows:

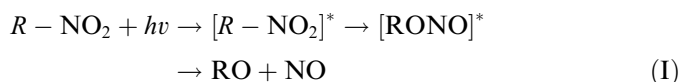
$$I_{J'} \propto \frac{N(J'', v'')}{2J'' + 1} S_{J', J''} \sum f(\tilde{\nu}_0 \tilde{\nu}_{\Delta v, v'', J'' \rightarrow J'})$$

where $I_{J'}$ is the intensity of fluorescence; $N(J'', v'')$ is the quantum number, $S_{J', J''}$ is the Hönl–London factor; $f(v_0, v) = \rho(v_0) \exp(-a(v_0 - v)^2)$ is the laser intensity distribution.

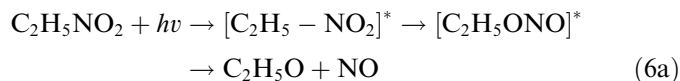
The rotational distribution of NO ($v'' = 0$) fragment from photodissociation of nitroethane can be described by Boltzmann distribution. The corresponding rotational temperature was obtained by fitting a straight line to a plot of $\ln[P(v'', J'')/(2J'' + 1)]$ vs $B_{v'', J''}(J'' + 1)$, where $B_{v'', J''}$ is the rotational constant. Fig. 2 shows the distribution of the rotational state populations of NO ($X^2\Pi_{1/2}$ and $X^2\Pi_{3/2}$) as a function of rotational energy (in the form of a Boltzmann plot) in the vibrational level of $v'' = 0$ following dissociation of nitroethane at 266 nm. From the relative intensity of several branches belonging to different spin components, we deduced the rotational-state distribution temperature for NO of $v'' = 0$ to be 810 ± 100 K within experimental uncertainty. Attempts to observe transitions due to $v'' = 1$ at 233–237 nm and higher vibrational levels of the NO fragment were unsuccessful. This suggests that majority of the NO fragment was formed in $v'' = 0$, indicating that the vibrational distribution did not have an anomalous maximum at some higher vibrational level. It had been found that in the photodissociation of other nitro-compound, such as nitrobenzene at 280–220 nm [8] and nitromethane at 193 nm [13], the NO fragments were also produced mainly in $v'' = 0$ state. The fact that NO product distributions are very similar for the different nitroalkanes shows that the rotational state distribution of NO is not strongly dependent on the structure of the nitroalkane. This is compatible with the participation of a common-lived intermediate state, rather than with a repulsive process.

One possible NO formation is through the isomerization of the nitroalkane ($R-NO_2$) into alkyl nitrite ($R-O-NO$)

followed by cleavage of the O–NO bond of the alkyl nitrite. Experimental evidence for unimolecular nitro-nitrite rearrangement, $R-NO_2 \rightarrow R-O-NO$, as an initial step in thermal decomposition had been reported in several nitro-compounds [2,3,7,8]. In general, nitro compounds photodissociation process that produces NO radical can be described as



Thus, for nitroethane,



We also used ab initio method to study the energetics of the nitroethane isomerization into ethyl nitrite. Fig. 3 shows the optimized geometry of nitroethane, ethyl nitrite and the transition state at MP2/6-31G** level of theory. In order to verify the transition state, we have performed the intrinsic reaction coordinate (IRC) for the isomerization process at

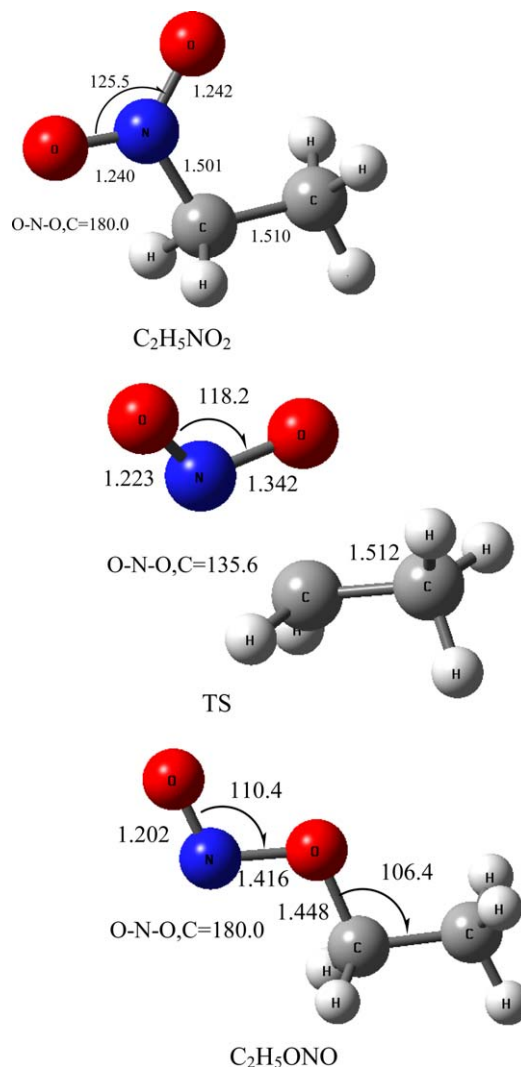


Fig. 3. Geometries optimized at the MP2/6-31G** level.

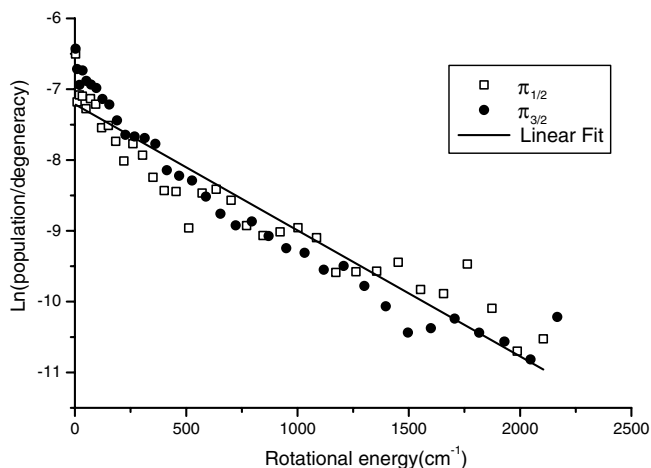


Fig. 2. NO($X^2\Pi$) $v'' = 0$ rotational state population as a function of rotational energy for photodissociation of $C_2H_5NO_2$ at 266 nm.

the MP2/6-31G** level and found that the transition state correlated to $\text{CH}_3\text{CH}_2\text{NO}_2$ and $\text{CH}_3\text{CH}_2\text{ONO}$ as reactant and product. We were unable to locate the transition state for ethyl nitrite dissociation into $\text{C}_2\text{H}_5\text{O} + \text{NO}$. It is not unusual that a closed shell molecule dissociates without involving a well defined transition state. The best estimate relative energy computed at MP4/6-311G**//MP2/6-31G** + ΔZPE level of theory for reaction (6a) is summarized in Fig. 4. Based upon our ab initio computational results, the heat of reaction (6a), $\Delta_r H^0(\text{reaction (6a)})$, is predicted to be $46.0 \text{ kcal mol}^{-1}$, which is about 10% higher than the experimental value of $42.0 \text{ kcal mol}^{-1}$. An activation energy barrier of $68.4 \pm 4.0 \text{ kcal mol}^{-1}$ is then estimated for the isomerization of nitroethane into ethyl nitrite based on our computational results. This value is higher by $8.6 \text{ kcal mol}^{-1}$ than that calculated by Denis et al. [35] using density functional methods. Since the C–N bond dissociation energy of $\text{CH}_3\text{CH}_2\text{NO}_2$ is ca. 61 kcal mol^{-1} [10,32,34], and the activation energy of molecular elimination decomposition (reaction (7), $\text{CH}_3\text{CH}_2\text{NO}_2 \rightarrow \text{C}_2\text{H}_4 + \text{HONO}$) has been reported to be $43 \pm 2 \text{ kcal mol}^{-1}$ [22], the nitroethane isomerization energy barrier of $68.4 \text{ kcal mol}^{-1}$ is higher than both the C–N bond dissociation energy and the molecular elimination ($\text{CH}_3\text{CH}_2\text{NO}_2 \rightarrow \text{C}_2\text{H}_4 + \text{HONO}$) activation energy. Therefore, the production of NO and ethoxy radicals from the photodissociation of nitroethane is estimated to be a minor channel comparing to the other two dissociation channels.

However, the NO might also be produced from further dissociation of NO_2 that is generated from reaction,



and it is difficult to experimentally distinguish the NO product from these two different reaction pathways. On the basis of available thermodynamic data [32–35], it has been documented that $\Delta_f H^0(\text{C}_2\text{H}_5\text{NO}_2) = -24.5 \text{ kcal mol}^{-1}$, $\Delta_f H^0(\text{C}_2\text{H}_5\text{ONO}) = -25.8 \text{ kcal mol}^{-1}$, $\Delta_f H^0(\text{C}_2\text{H}_5\text{O}) = -4.1 \text{ kcal mol}^{-1}$, $\Delta_f H^0(\text{C}_2\text{H}_5) = 28.4 \text{ kcal mol}^{-1}$, $\Delta_f H^0(\text{NO}) = 21.6 \text{ kcal mol}^{-1}$, $\Delta_f H^0(\text{NO}_2) = 7.9 \text{ kcal mol}^{-1}$, and $\Delta_f H^0(\text{O}) = 59.6 \text{ kcal mol}^{-1}$. This leads to $\Delta_r H^0(\text{reaction (6a)}) = 42.0 \text{ kcal mol}^{-1}$, and $\Delta_r H^0(\text{reaction (4a)}) = 134.1 \text{ kcal mol}^{-1}$, respectively. Reaction (6a) is then less endothermic than reaction (4a) and should be more thermodynamically favored than reaction (6a). However, assuming reaction (4a) has no activation energy barrier [35], whether the reaction (6a) is kinetically favored or not will depend on the activation energy barrier associated with the isomerization of nitroethane into ethyl nitrite. On the basis of our calculation results, the photon energy at 266 nm ($107.4 \text{ kcal mol}^{-1}$) absorbed by the nitroethane will be sufficient to allow reaction (6a) to occur. The photon energy is also sufficient for production of C_2H_5 and NO_2 , but not sufficient for production of $\text{C}_2\text{H}_5 + \text{O} + \text{NO}$, which requires $134.1 \text{ kcal mol}^{-1}$. Therefore, reaction (6a) is considered to be both thermodynamically and kinetically more favored than reaction (4a) for production of NO. Additionally, the NO might also be produced through reaction (7) and (8). Although the activation energy of the ($\text{C}_2\text{H}_4 + \text{HONO}$) elimination channel via an intramolecular rearrangement is relatively lower ($43 \pm 2 \text{ kcal mol}^{-1}$), the subsequent HONO dissociation energy to produce the NO product is 48 kcal mol^{-1} , while the dissociation energy of $[\text{C}_2\text{H}_5\text{ONO}]^* \rightarrow \text{C}_2\text{H}_5\text{O} + \text{NO}$ is $43.3 \text{ kcal mol}^{-1}$.

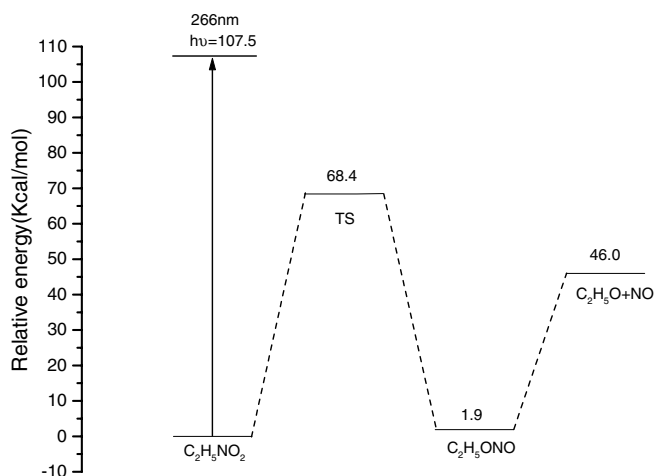
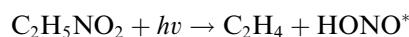
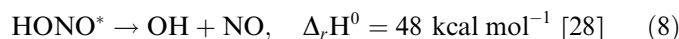


Fig. 4. Relative energy diagram for the nitroethane isomerization to ethyl nitrite calculated at the MP4/6-311G**//MP2/6-31G** + ΔZPE level of theory.

$\text{H}_5\text{O}) = -4.1 \text{ kcal mol}^{-1}$, $\Delta_f H^0(\text{C}_2\text{H}_5) = 28.4 \text{ kcal mol}^{-1}$, $\Delta_f H^0(\text{NO}) = 21.6 \text{ kcal mol}^{-1}$, $\Delta_f H^0(\text{NO}_2) = 7.9 \text{ kcal mol}^{-1}$, and $\Delta_f H^0(\text{O}) = 59.6 \text{ kcal mol}^{-1}$. This leads to $\Delta_r H^0(\text{reaction (6a)}) = 42.0 \text{ kcal mol}^{-1}$, and $\Delta_r H^0(\text{reaction (4a)}) = 134.1 \text{ kcal mol}^{-1}$, respectively. Reaction (6a) is then less endothermic than reaction (4a) and should be more thermodynamically favored than reaction (6a). However, assuming reaction (4a) has no activation energy barrier [35], whether the reaction (6a) is kinetically favored or not will depend on the activation energy barrier associated with the isomerization of nitroethane into ethyl nitrite. On the basis of our calculation results, the photon energy at 266 nm ($107.4 \text{ kcal mol}^{-1}$) absorbed by the nitroethane will be sufficient to allow reaction (6a) to occur. The photon energy is also sufficient for production of C_2H_5 and NO_2 , but not sufficient for production of $\text{C}_2\text{H}_5 + \text{O} + \text{NO}$, which requires $134.1 \text{ kcal mol}^{-1}$. Therefore, reaction (6a) is considered to be both thermodynamically and kinetically more favored than reaction (4a) for production of NO. Additionally, the NO might also be produced through reaction (7) and (8). Although the activation energy of the ($\text{C}_2\text{H}_4 + \text{HONO}$) elimination channel via an intramolecular rearrangement is relatively lower ($43 \pm 2 \text{ kcal mol}^{-1}$), the subsequent HONO dissociation energy to produce the NO product is 48 kcal mol^{-1} , while the dissociation energy of $[\text{C}_2\text{H}_5\text{ONO}]^* \rightarrow \text{C}_2\text{H}_5\text{O} + \text{NO}$ is $43.3 \text{ kcal mol}^{-1}$.



$$\Delta_r H^0 = 18.6 \text{ kcal mol}^{-1} \quad [24] \quad (7)$$



Reaction (8) only produces NO when the nascent HONO produced via reaction (7) contains energy in excess of 48 kcal mol^{-1} . In the photodissociation of 1-nitropropane at 282 nm, Haas and coworkers [24] found the quantum yield of NO from HONO elimination and dissociation is small by a factor of 5 than the OH yield.

Thus, the photodissociation mechanism resulting in NO production of nitroethane is then proposed as follows. In a minor reaction pathway, after the parent nitroethane molecule absorbed a photon at 266 nm ($107.5 \text{ kcal mol}^{-1}$), $68.4 \text{ kcal mol}^{-1}$ of the energy was used to cross the barrier of the transition for isomerization to ethyl nitrite, the remaining energy was then contributed to $\text{CH}_3\text{CH}_2\text{ONO}$ decomposition to yield $\text{C}_2\text{H}_5\text{O}$ and NO radicals. Although the isomerization process is not a favored dissociation channel of nitroethane, most of the NO product is produced from this channel. Our observation of the vibrationally cold, Boltzmann rotational distribution of the NO fragment suggests that a relatively high degree of internal excitation for the $\text{C}_2\text{H}_5\text{O}$ fragment is anticipated.

4. Conclusion

We have probed the internal-state distribution of the $\text{NO}(X^2\Pi)$ fragment after photodissociation from nitro-

ethane at 266 nm using the one-photon laser-induced fluorescence (LIF) technique. The observed NO $v'' = 0$ state fragment is vibrationally cold and the rotational distribution can be characterized by Boltzmann temperature of 810 ± 100 K. Ab initio calculation results suggest that the NO may be produced from a two-step process in the photodissociation of nitroethane, in which the nitroethane is first isomerized into ethyl nitrite followed by dissociation of the ethyl nitrite. This is based on the prediction of a barrier height of $68.4 \text{ kcal mol}^{-1}$ for isomerization of nitroethane to ethyl nitrite.

Acknowledgements

This work was supported by NKBRFSF (Grant 1999075302) and NSFC (Grants 20373071, 20333050).

References

- [1] P. Axson Roberta, M. Yoshimine, *Can. J. Chem.* 70 (1992) 572.
- [2] A.M. Wodtke, E.J. Hints, Y.T. Lee, *J. Chem. Phys.* 84 (1986) 1044.
- [3] A.M. Wodtke, E.J. Hints, Y.T. Lee, *J. Phys. Chem.* 90 (1986) 3549.
- [4] L.J. Butler, D. Krajnovich, Y.T. Lee, G. Ondrey, R. Bersohn, *J. Chem. Phys.* 79 (1983) 1708.
- [5] C. Kosmidis, K.W.D. Ledingham, A. Clark, A. Marshall, R. Jennings, J. Sander, R.P. Singhal, *Int. J. Mass Spectrom. Ion Proc.* 135 (1994) 229.
- [6] M.S. Park, K.-H. Jung, H.P. Upadhyaya, H.-R. Volpp, *Chem. Phys.* 270 (2001) 133.
- [7] D.B. Galloway, T.G. Meyer, J. Bartz, L.G. Huey, F.F. Crim, *J. Chem. Phys.* 100 (1994) 1946.
- [8] D.B. Galloway, J.A. Barta, L.G. Huey, F.F. Crim, *J. Chem. Phys.* 98 (1993) 2107.
- [9] G.-M. Thomas, F.F. Crim, *J. Mol. Struct. (Theochem)* 337 (1995) 209.
- [10] M.L. McKee, *Chem. Phys. Lett.* 164 (1989) 520.
- [11] A.F. Tuck, *J. Chem. Soc. Faraday Trans. II* 73 (1977) 689.
- [12] H.L. Gregory, Ph.D.thesis, University of Wisconsin–Madison, 1992.
- [13] D.B. Moss, K.A. Trentelman, P.L. Houston, *J. Chem. Phys.* 96 (1992) 237.
- [14] N.C. Blais, *J. Chem. Phys.* 79 (1983) 1723.
- [15] J.C. Mialocq, J.C. Stephenson, *Chem. Phys.* 106 (1986) 281.
- [16] Y.L. Chow, in: S. Patai (Ed.), *The Chemistry of Amino, Nitroso and Nitrocompounds and their Derivatives*, Suppl. F, Part 1, Wiley, New York, 1982.
- [17] G.H. Penner, *J. Mol. Struct. (Theochem)* 137 (1986) 121.
- [18] K.Q. Lao, E. Jensen, P.W. Kash, L.J. Butler, *J. Chem. Phys.* 93 (1990) 3958.
- [19] W. Tsang, D. Robaugh, W.G. Mallard, *J. Phys. Chem.* 90 (1986) 5968.
- [20] M.J.S. Dewar, J.P. Ritchie, J. Alster, *J. Org. Chem.* 50 (1985) 1031.
- [21] B.H. Rockney, E.R. Grant, *J. Chem. Phys.* 79 (1983) 708.
- [22] G.N. Spokes, S.W. Benson, *J. Am. Chem. Soc.* 89 (1967) 6030.
- [23] M.J.S. Dewar, W. Thiel, *J. Am. Chem. Soc.* 99 (1977) 4899.
- [24] G.D. Greenblatt, H. Zuckerman, Y. Haas, *Chem. Phys. Lett.* 134 (1987) 593.
- [25] S. Zabarnick, J.W. Fleming, A.P.J. Baronawski, *Chem. Phys.* 85 (1986) 3395.
- [26] K.G. Spears, S.P. Brugge, *Chem. Phys. Lett.* 54 (1978) 373.
- [27] H.S. Kwok, G.Z. He, R.K. Sparks, Y.T. Lee, *Int. J. Chem. Kinet.* 13 (1981) 1125.
- [28] G. Radhakrishnan, T. Parr, C. Wittig, *Chem. Phys. Lett.* 111 (1984) 25.
- [29] J.C. Mialocq, J.C. Stephenson, *Chem. Phys.* 106 (1986) 281.
- [30] M.J. Frisch et al., *GAUSSIAN98*, Version 5.4, Revision A.9, Gaussian Inc., Pittsburgh, PA, 1998.
- [31] G. Herzberg, *Molecular Spectra and Molecular Structure Electronic Spectra and Electronic Structure of Polyatomic Molecules*, vol. III, Van Nostrand, Princeton, 1966, p. 483.
- [32] D.R. Lide, *CRC Handbooks of Chemistry and Physics*, 82nd ed., 2001–2002.
- [33] R.E. Rebert, K.J. Laidler, *J. Chem. Phys.* 20 (1952) 574.
- [34] S.P. Sander, R.R. Friedl, D.M. Golden, M.J. Kurylo, R.E. Huie, V.L. Orkin, G.K. Moortgat, A.R. Ravishankara, C.E. Kolb, M.J. Molina, B.J. Finlayson–Pitts, *Chemical Kinetics and Photochemical Data for Use in Stratospheric Modeling*, JPL Publication, 02–25, 2003.
- [35] P.A. Denis, O.N. Ventura, H.T. Le, M.T. Nguyen, *Phys. Chem. Chem. Phys.* 5 (2003) 1730.